PCCP

PAPER

View Article Online
View Journal | View Issue

Cite this: *Phys. Chem. Chem. Phys.*, 2016, **18**, 9816

Complexation thermodynamics of diglycolamide with f-elements: solvent extraction and density functional theory analysis†

Sk. M. Ali,*[a] S. Pahan,[b] A. Bhattacharyya[c] and P. K. Mohapatra[c]

Received 5th February 2016,
Accepted 9th March 2016

DOI: 10.1039/c6cp00825a

www.rsc.org/pccp

Comparative extraction of trivalent lanthanide and actinide ions (La^{3+}, Eu^{3+}, Lu^{3+}, Am^{3+} and Cm^{3+}) with tetra-*n*-octyl diglycolamide (TODGA) was studied and showed the trend: $Lu^{3+} > Eu^{3+} > Cm^{3+} > Am^{3+} > La^{3+}$. The structure, bonding, energetic and thermodynamic parameters of the trivalent lanthanide and actinide ions (La^{3+}, Eu^{3+}, Lu^{3+}, Am^{3+} and Cm^{3+}) with a tridentate ligand, tetra-methyl diglycolamide (TMDGA), are reported in the gas and solvent phases in order to understand their complexation and extraction behaviour. The calculations were performed using the generalized gradient approximated BP86 density functional and the hybrid B3LYP functional using SVP and TZVPP basis sets. The calculated structure obtained at the BP86/SVP level of optimization was found to be in close agreement with the X-ray data and also with the structure obtained at the B3LYP/TZVP level of theory. The free energy of extraction was found to be exergonic for the explicit monomer water model. From the solvent extraction experiment the order of extraction was observed as $Lu^{3+} > Eu^{3+} > Cm^{3+} > Am^{3+} > La^{3+}$, which was in line with the trends predicted based on the free energy changes in the gas phase calculations (ΔG_{gp}). The Born–Haber thermodynamic cycle and the COSMO (conductor like screening model) solvation model were applied to calculate the free energy of extraction, ΔG_{ext}, of lanthanide and actinide ions in the aqueous–dodecane biphasic system and ΔG_{ext}, however, predicted different extraction trends. After dispersion correction (B3LYP-D3), the free energy of extraction for the metal ions was found to follow the order: $Lu^{3+} > Eu^{3+} > La^{3+}$, which was also observed in the solvent extraction experiments. Both COSMO and DCOSMO-RS models predict the same metal ion selectivity trend. Different bonding analyses indicate the electrostatic and less covalent nature of interactions between the ligands and the metal ions.

Introduction

'Actinide partitioning', considered as a key step in the proposed high level waste (HLW) management, requires the selective extraction of minor actinides from a mixture of a host of fission and activation products in 3–4 M HNO_3.[1] Several processes such as TRUEX,[2] TRPO,[3] DIDPA,[4] DIAMEX[5] have been developed for this purpose using CMPO (octyl(phenyl)-*N*,*N*′-diisobutyl-carbamoylmethyl phosphine oxide), TRPO (tri-*n*-alkyl phosphine oxides), DIDPA (diisodecylphosphoric acid), and DMDOHEMA

[a] *Chemical Engineering Division, Bhabha Atomic Research Centre, Trombay, Mumbai-400085, India. E-mail: musharaf@barc.gov.in; Fax: +91-2505151; Tel: +91-25591992*
[b] *Process Developement Division, Bhabha Atomic Research Centre, Trombay, Mumbai-400085, India*
[c] *Radiochemistry Division Bhabha Atomic Research Centre, Trombay, Mumbai-400085, India. E-mail: mpatra@barc.gov.in*

† Electronic supplementary information (ESI) available: Details of computational methodology, structural, interaction and thermodynamical parameters. Fig. S1: the calculated structure and energy of conformers of TMDGA and its complexes with Eu^{3+} ions at the BP/SVP level of theory, Table S1: slope values obtained from the TODGA concentration variation experiments in *n*-dodecane medium, Tables S2 and S3: structural parameters of 1 : 1 and 1 : 2 stoichiometric complexes. Table S4: binding energies for different stoichiometric complexes. Tables S5, S6 and S7: thermodynamic parameters for different models. Table S8: NPA analysis, Table S9: AIM parameters for $M(DGA)_3$ and aqua complexes. Table S10: second order stabilization energies of $M(DGA)_3$ complexes, Table S11: calculated values of reaction enthalpy, entropy and free energies in the gas phase and in solution. Table S12: calculated values of thermodynamic parameters of different Ln–An complexes in the presence of nitrate ions using the monomer water model, Table S13: calculated values of thermodynamic parameters of different Ln–An complexes in the presence of nitrate ions using the cluster water model, Table S14: calculated values of the thermodynamic parameters of Ln–An complexes in the presence of nitrate anions using monomer water + DCOSMO-RS, Table S15: calculated values of the thermodynamic parameters of Ln–An complexes in the presence of nitrate anions using cluster water + DCOSMO-RS, Table S16: calculated values of the thermodynamic parameters of Ln in the presence of nitrate anions using cluster water + DCOSMO-RS at the B3LYP-D3 level of theory, and Table S17: calculated total energy and stabilization energy of the various conformers of TMDGA, the total energy of the Eu^{3+}–TMDGA complex with conff (with tridentate donor O atoms) and with the most stable conformer, conf0 and the corresponding binding energy at the BP/SVP level of theory. See DOI: 10.1039/c6cp00825a

(*N*,*N*′-dimethyl-*N*,*N*′-dioctyl-2-hexylethoxy-malonamide) as the extractants selective for the minor actinide ions. Recent studies with diglycolamides (DGA) such as TODGA (*N*,*N*,*N*′,*N*′-tetra-*n*-octyl diglycolamide) indicated this class of extractants to be the most promising.[6] Though there are numerous studies on the extraction of actinide ions with the DGA based extractants such as TODGA[6] and its homologs such as T2EHDGA[7] (*N*,*N*,*N*′,*N*′-tetra-2-ethylhexyl diglycolamide) and the unsymmetrical diglycolamides,[8] structural studies with their actinide/lanthanide complexes are very limited. The complexes of DGA ligands with longer alkyl chains such as *n*-octyl (as in TODGA) or 2-ethylhexyl (as in T2EHDGA) are usually difficult to crystallize and hence, lower homologs have been used in the reported structural studies. Kannan *et al.* reported the X-ray crystal structures of the complexes of UO_2^{2+} and La^{3+} with TiPrDGA (*N*,*N*,*N*′,*N*′-tetra-*iso*-propyl diglycolamide) and TiBuDGA (*N*,*N*,*N*′,*N*′-tetra-*iso*-butyl diglycolamide), respectively.[9] More recently, X-ray crystal structures of the homoleptic complexes of NpO_2^+ and Pu(IV) with TMDGA (*N*,*N*,*N*′,*N*′-tetra-methyl diglycolamide) have been reported.[10] Apart from the X-ray crystal structure reports, there are very few reports on the EXAFS studies on the complexes of lanthanides (considered as surrogates of the trivalent actinides) with DGA ligands.[11] Narita *et al.* from their EXAFS studies reported two types of M–O bonds, carbonyl as well as etheric (2.33 Å and 2.47 Å, respectively), and Antonio *et al.*[11b] reported nine M–O bonds (no distinction was made between the carbonyl and etheric 'O' atoms) at *ca.* 2.40 Å.

The structural information can be obtained from the theoretical calculations using the DFT (density functional theory) methods. Though there are many theoretical studies available on the separation of actinides from lanthanides,[12] only a handful of reports are available on the complexation involving DGA ligands. There are theoretical studies on the complexation of trivalent lanthanides and actinides with DGA ligands.[13] Wang *et al.*[13a] considered 1 : 1 and 1 : 2 species neglecting the commonly reported 1 : 3 (or even 1 : 4) extracted species and suggested the preferential extraction of Am(III) as compared to Eu(III) which is just the opposite of the observed trend. The calculated results do not conform to the experimental results which may be due to the consideration of inaccurate complexation stoichiometry. A more recent publication by Narbutt *et al.*[13b] reported the free energy of extraction for Eu(III) and Am(III) with TEDGA (used as a TODGA homolog) in an organic solvent which is of less experimental interest. Moreover, they have not included the counter anion (*viz.* nitrate) in the calculations, which might lead to differences between the calculated and experimental results. Though there are very limited structural studies involving the diglycolamide complexes of lanthanides and actinides using X-ray crystallography,[9,10] EXAFS,[11] and computations,[13] a thorough investigation involving the solvent extraction and computational study is lacking. In view of the potential application of DGA ligands for the radioactive waste remediation and their intriguing complexation behaviour, we have undertaken an extensive and systematic investigation in this paper to study the complexation reaction of DGA with the f elements by analysing the structure, bonding, energetic and thermodynamical parameters using the DFT calculations. Furthermore, the computational studies reported by Narbutt *et al.*[13b] considered the correct stoichiometry that did not accommodate the presence of the counter anions (nitrate). In view of this, we have performed a detailed DFT based investigation which accounts not only the correct stoichiometry but also the presence of counter anions and a realistic organic solvent (*n*-dodecane). In view of a wealth of data being available in the literature on the extraction of trivalent lanthanide/actinide ions using DGA ligands, the solvent extraction studies were limited to the bare minimum in this paper and were only carried out to give comparative distribution coefficient data under given experimental conditions.

Experimental section

Solvent extraction studies

Reagents and chemicals. TODGA was synthesized following the procedure described elsewhere[6d] and characterized by elemental analysis, melting point and NMR (^{1}H as well as ^{13}C) spectral analysis. Laboratory stock solutions of ^{241}Am and ^{244}Cm were used for studies involving the actinides after checking their radiochemical purity by alpha-spectrometry. ^{152}Eu and ^{154}Eu, procured from the Board of Radiation and Isotope Technology (BRIT), Mumbai, India, were used after ascertaining their radiochemical purity by gamma ray spectrometry. ^{140}La and ^{177}Lu were prepared by irradiating their respective natural isotopes in a Dhruva reactor at a neutron flux of 10^{13} n cm^{-2} s^{-1}. Suprapur nitric acid (Merck) and MilliQ water (Millipore) were used for preparing the tracer solutions.

Distribution studies. Distribution studies were carried out with ^{241}Am, ^{244}Cm, ^{140}La, ^{177}Lu and ^{152,154}Eu as the tracers spiked in aqueous solutions containing 1 M nitric acid. The organic phases were prepared by dissolving varying concentrations of TODGA in *n*-dodecane (Lancaster). Equal volumes (1 mL) of the organic and the aqueous phases were taken in a leak-tight stoppered tube and agitated in a thermostated water bath at 25 ± 0.1 °C for 2 h. The tubes were subsequently centrifuged and suitable aliquots (0.1 mL) were taken from both the phases followed by their radiometric assay by gamma ray counting using a well type NaI(Tl) scintillation detector (Para Electronics) coupled to a multi-channel analyzer (ECIL, India). The distribution ratio (*D*) was calculated as the ratio of counts per minute of the corresponding radiotracer per unit volume in the organic phase to that in the aqueous phase. The material balance was within the error limits of ±5%.

Computational protocols. The minimum energy structures of tetra methyl DGA (TMDGA) and tetra-*iso*-butyl DGA (TiBDGA) and their complexes with the trivalent lanthanides (La^{3+}, Eu^{3+} and Lu^{3+}) and actinides (Am^{3+} and Cm^{3+}) were calculated using the GGA based BP86[14] functional employing the split valence plus polarization (SVP) basis set[15] as available in the Turbomole suite of programs.[16] In the case of La^{3+}, Eu^{3+}, Lu^{3+}, Am^{3+} and Cm^{3+}, an ECP core potential was used, where 46 electrons are kept in the core of La[17] and 28 electrons are kept in the core of

Eu[18] and Lu[19] respectively, whereas the number of core electrons was 60 for the Am and Cm[20] elements respectively. The default ECP available for La in Turbomole is 46 electrons in the core, which is considered to be a large core ECP, whereas if one wants to include the orbital for $n = 4$, then the core electrons will be 28. Here, we use the non-relativistic DFT and the relativistic effect is inducted through ECP. For large core ECP, the account of relativistic effect is high but the account of all-electron effect is small, whereas for small core ECP, contribution of all-electron effect is high but the account of relativistic effect is small. This should make no appreciable difference when comparing relative energies but absolute energies may thus differ. Furthermore, there is no optimized basis set for the La which is compatible with the ECP-28 in Turbomole package. Moreover, the spatial extent of the 4f orbital of Eu and Lu is small; making them to a certain level core like and hence the ECPs can be used for calculating the molecular properties with reasonable accuracy.[21] Despite the fact that the BP86 functional is quite faster and accurate in predicting the geometry and vibrational frequencies,[22] the energetic parameters are not accurate enough compared to the hybrid functional due to non-consideration of the non-local HF part in the exchange functional. Therefore, the total energies were calculated using the B3LYP functional[23] employing the triple zeta valence plus double polarization (TZVPP) basis set[24] using equilibrated structures obtained at the BP86/SVP level of theory. The hybrid B3LYP (Becke''s three-parameter nonlocal hybrid exchange correlation functional, Becke–Lee–Yang–Parr) functional was found to be superior in the prediction of the energetic parameters due to the inclusion of the non-local HF contribution in the exchange functional.[23b] The optimization of the complexes with Eu^{3+} and Am^{3+} was performed using the septet spin state and for Cm^{3+}, the octet spin state was considered. There are numerous literature reports where the BP86 and B3LYP functionals have been used for the calculation of molecular properties of high spin Eu and Am systems. Hence, DFT was selected for the calculations of the present Eu and Am systems. The issue of degeneracy due to spin is generally checked by comparing the value of $\langle S^2 \rangle$ and $(S + 1)$. In the present chemical system, the value of $\langle S^2 \rangle$ is found to be very close to the $(S + 1)$ ideal values which indicates that all the chemical structures display negligible spin contamination. The COSMO solvation scheme was used to account for the solvent effects on the energetic parameters.[25] The default COSMO radii were used for all the elements except for La^{3+}, Eu^{3+}, Lu^{3+} Am^{3+} and Cm^{3+} for which the values of COSMO radii used were 2.03, 1.90, 1.79, 1.99 and 1.95 Å, respectively. The dielectric constants, ε of 80 and 1.8, were used to represent water and dodecane, respectively. The computation of solvation energy for the metal ions in water was performed using the monomer and cluster water explicit solvation models.

Results and discussion

Solvent extraction studies

Extraction of various trivalent actinide and lanthanide ions, *viz.* Am^{3+}, Cm^{3+}, La^{3+}, Eu^{3+} and Lu^{3+} was carried out from 1 M HNO_3 medium using 0.1 M TODGA solution in *n*-dodecane. The results are listed in Table 1, which shows an increase in the distribution ratio values with increasing atomic number in a particular series (actinide or lanthanide).

Table 1 Extraction behaviour of An^{3+} and Ln^{3+} with 0.1 M TODGA/*n*-dodecane in 1 M HNO_3 medium

M^{3+}	D_M[a]	D_M[b]	M^{3+}	D_M[a]	D_M[b]
La^{3+}	5.3 ± 0.2	5.3	Am^{3+}	25.7 ± 0.5	30
Eu^{3+}	190 ± 10	265	Cm^{3+}	71 ± 1	78
Lu^{3+}	1020 ± 30	631	—	—	

[a] Present work. [b] Ref. 26.

This could be explained on the basis of increasing ionic potential with increasing atomic number in a series. The distribution ratio values follow the order $D_{Lu} > D_{Eu} > D_{Cm} > D_{Am} > D_{La}$. In order to identify the extractable species, La^{3+} and Lu^{3+} extraction studies were carried out varying the TODGA concentration from 0.02 to 0.1 M (Fig. 1). From the slope analysis, 1 : 3 (M : L) extracted species were ascertained for both the lanthanide ions, which was in line with that reported for the other metal ions (slope analysis data for La^{3+} and Lu^{3+} are listed in Table S1, (ESI†) along with the respective reported values for Cm^{3+}, Am^{3+} and Eu^{3+}).[26] This suggested that the extraction equilibrium can be given as:

$$M^{3+}_{(aq)} + 3TODGA_{(org)} + 3NO_3^-{}_{(aq)} \leftrightarrow M(NO_3)_3 \cdot 3TODGA_{(org)} \quad (1)$$

where, the species with the subscripts '(aq)' and '(org)' refer to the species present in the aqueous and organic phases, respectively. Though the extracted species contained 3 TODGA molecules, the mode of coordination of the 'O' atoms was required to be understood for which theoretical studies were carried out.

Computational studies

Structural parameters. The optimized minimum energy structures of TMDGA and TiBDGA ligands are displayed in Fig. 2. It is seen that in TMDGA as well as TiBDGA, all the donor O atoms are pointed to the same direction and in the same plane.

Very similar C═O, C–O (O atom of the ether link) and C–N bond distances were observed in the cases of TMDGA and TiBDGA. In order to test the accuracy of the BP86/SVP level of calculation in the prediction of the geometry of metal ion–ligand

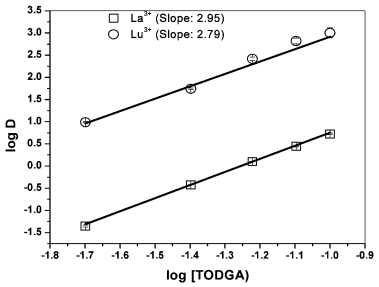

Fig. 1 Effect of TODGA concentration on the distribution ratio of La^{3+} and Lu^{3+}; Org. phase: TODGA in *n*-dodecane; Aq. phase: 1 M HNO_3.

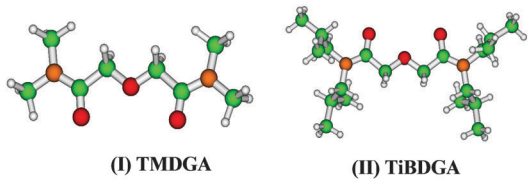

Fig. 2 The optimized minimum energy structures of free TMDGA and TiBDGA at the BP/SVP level of theory. Red, green, yellow and grey sphere represent the O, C, N and H atoms, respectively.

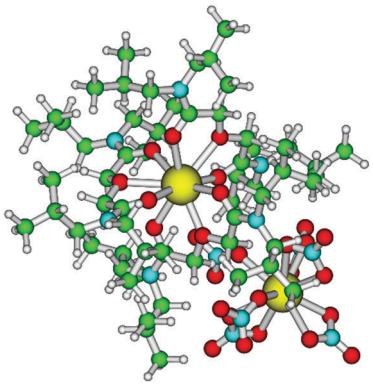

Fig. 3 Optimized structures of the La^{3+} metal ion complex with TiBDGA in a 2 : 3 stoichiometry (M : L) at the BP/SVP level of theory. The key is same as in Fig. 1.

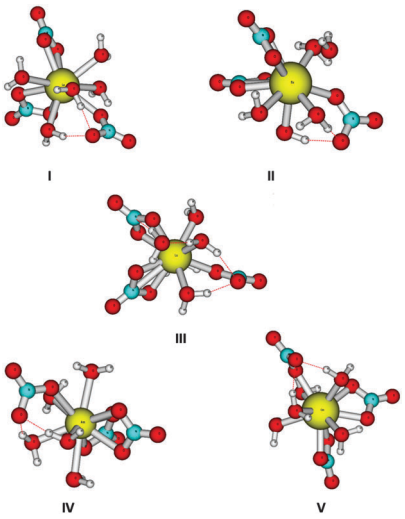

Fig. 4 Optimized structures of the metal ion complexes with nitrate anions in a 1 : 3 stoichiometry at the BP/SVP level of theory with 5 coordinating water molecules. The key is same as in Fig. 1. (I) La^{3+}; (II) Eu^{3+}; (III) Lu^{3+}; (IV) Am^{3+}; (V) Cm^{3+}.

complexes, we have optimized a TiBDGA coordinated La^{3+} ion in 2 : 3 stoichiometry (M : L). The calculated structural parameters of the optimized structure (Fig. 3) are compared with the X-ray data[9] (Table 2) as commonly practiced.[12b,27,28]

From Fig. 3, it is noticed that in the optimized structure, one La^{3+} ion was found to be coordinated to 9 O atoms of 3 TiBDGA units in a distorted tricapped trigonal prismatic fashion, whereas another La^{3+} ion was coordinated to 6 nitrate ions. It is interesting to note that in the computed structure of the $La(TiBDGA)_3^{3+}$ complex, the metal ion has ten-fold coordination (9 from 3 TiBDGA ligands and one from the nitrate anion), whereas nine-fold coordination (9 O atoms from 3 TiBDGA ligands) was reported from an X-ray study, though the initial coordinates of X-ray data were used in the optimization. On the other hand, computations suggested 4 nitrates as bidentate ligands and the remaining two as monodentate ligands, leading to a deca-coordination for the $La(NO_3)_6^{3-}$ complex, whereas the X-ray structural report suggested a dodeca-coordination with all the six nitrates acting as bidentate ligands.

The change in the bond distance of C═O, C–O (O atom of the ether link) and C–N of a free TiBDGA ligand was found to be 0.01 Å, 0.001 Å and 0.01 Å, respectively, after complexation with the La^{3+} metal ion. The calculated average M–O bond distance was found to be within 0.07 Å (O of C═O), 0.1 Å (ether O) and 0.04 Å (O of NO_3) with the average bond distance reported from X-ray data. The structural parameters calculated using the BP/SVP level of theory is quite close to the structural parameters predicted using the X-ray study. The optimized structures of hydrated metal ion–nitrate complexes (1 : 3) of La^{3+}, Eu^{3+}, Lu^{3+}, Am^{3+} and Cm^{3+} are displayed in Fig. 4, where all the three nitrate ions are found to be not coordinated in bidentate mode due to the presence of water molecules. Two nitrate ions are found to be coordinated to the metal ion in a bidentate mode and one nitrate ion in monodentate mode, whereas all five water molecules are directly coordinated to the metal ion leading to 10 fold coordination. The calculated structural parameters are listed in Table 3. The M–O (O of NO_3) was found to be shorter than the M–O (O of H_2O) bond length for all the metal ions studied here. The value of the M–O bond distance for the hydrated metal ion–nitrate complex of La^{3+} reported in the X-ray analysis is also presented in the same table. The calculated average bond distance was found to be within 0.24 Å (O of NO_3) and 0.06 Å (O of H_2O) from the reported X-ray results.[29] Next, the optimized structures of metal ion–diglycolamide ligand complexes along with nitrate ions (1 : 3) are displayed in Fig. 5.

The calculated structural parameters are listed in Table 4. The metal ion was found to be nine-fold coordinated: 9 donor O

Table 2 Calculated structural parameters (in Å) of the La^{3+}–$(TiBDGA)_3$ complex along with the X-ray crystallographic data[9] (in parentheses)

	M–O		
C═O	(O of C═O)	(ether O)	(O of NO_3)
1.25, 1.25, 1.27, 1.28, 1.25, 1.26 (1.25, 1.24, 1.24, 1.25, 1.25, 1.24)	2.62, 2.49, 2.62, 2.63, 2.52, 2.53 (2.49, 2.49, 2.50, 2.49, 2.50, 2.49)	2.77, 2.50, 2.77 (2.57, 2.58, 2.58)	2.66, 2.76, 2.55, 2.57, 2.65, 2.61, 2.68, 2.66, 2.67, 2.67 (2.66, 2.71, 2.71, 2.64, 2.64, 2.66, 2.60, 2.71, 264, 2.66, 2.64, 2.60)

Table 3 Calculated structural parameters (Å) of the M–$(NO_3)_3$ complex at the BP/SVP level of theory

	$M–(NO_3)_3–(H_2O)_5$		
Metals	M–O (O of NO_3)	M–O (O of H_2O)	$M–(NO_3)_3$
La	2.58, 2.59, 2.60, 2.62, **2.62** (2.62, 2.85, 2.66, 2.88, 2.69, 2.70)	2.64, 2.61, 2.58, 2.65, 2.71 (2.66, 2.58, 2.56, 2.56, 2.52)	2.50, 2.50, 2.50, 2.50, 2.49, 2.50
Eu	2.51, 2.51, 2.50, 2.48, **2.52**	2.48, 2.53, 2.60, 2.53, 2.62	2.39, 2.39, 2.40, 2.38, 2.39, 2.39
Lu	2.34, 2.36, 2.37, 2.37, **2.36**	2.38, 2.40, 2.39, 2.29, 3.46	2.24, 2.24, 2.24, 2.24, 2.24, 2.24
Am	2.49, 2.49, 2.54, 2.50, **2.55**	2.55, 2.57, 2.52, 2.63, 2.54	2.37, 2.38, 2.39, 2.39, 2.38, 2.38
Cm	2.50, 2.50, 2.49, 2.47, **2.51**	2.54, 2.54, 2.49, 2.64, 2.65	2.38, 2.37, 2.39, 2.37, 2.38, 2.37

Values in the parentheses represent the experimental results.[29] Bold data represent the nitrate anions in monodentate coordination.

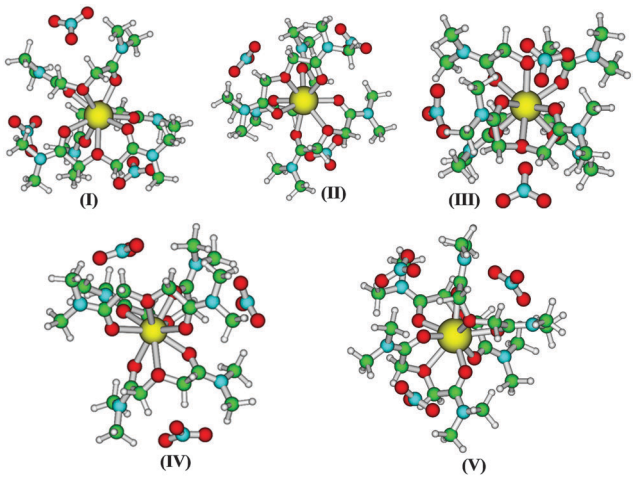

Fig. 5 Optimized structures of the metal ion complexes with TMDGA in a 1 : 3 stoichiometry at the BP/SVP level of theory in the presence of nitrate anions. The key is same as in Fig. 1. (I) La^{3+}; (II) Eu^{3+}; (III) Lu^{3+}; (IV) Am^{3+}; (V) Cm^{3+}.

atoms from 3 units of TMDGA. The three nitrate ions were located outside the first sphere of coordination to satisfy the charge neutrality of the metal ion complex to enable it to be transferred in the dodecane phase. In the complexes of metal ions, (La^{3+}, Eu^{3+}, Lu^{3+}, Am^{3+} and Cm^{3+}) the average M–O (O atom of C=O) bond distance was found to be lengthened compared to the bond distance observed in the absence of nitrate ions (Table 5) and the bond distance follows the order $La^{3+} > Eu^{3+} > Am^{3+} > Cm^{3+} > Lu^{3+}$. The M–O (O atom of C=O) bond distance was found to be shorter than the M–O (O atom of ether link) bond distance.

The M–O (O of nitrate) bond distance was found to be shorter than that of M–O (O atom of C=O) and the M–O (O atom of ether link) bond distance due to the 'pulling effect' of the nitrate ion on the central metal ion. In complexes of the metal ions (La^{3+}, Eu^{3+}, Lu^{3+}, Am^{3+} and Cm^{3+}) the C=O and C–O bond distances were found to be shortened, whereas the C–N bond distance was found to be lengthened slightly compared to the respective 1 : 3 stoichiometric complexes without nitrate ions. The calculated structural parameters are listed in Table 5. In complexes of the metal ions (La^{3+}, Eu^{3+}, Lu^{3+}, Am^{3+} and Cm^{3+}) with DGA, the C=O and C–O bond distances were found to be lengthened, whereas the C–N bond distance was found to be shortened substantially compared to those in the free ligand. Also, the bond distances were found to be lengthened compared to 1 : 1 and 1 : 2 stoichiometric complexes (Tables S2 and S3, ESI†).

The optimized structures of the M^{3+}–DGA complexes without nitrate ions (1 : 3) are displayed in Fig. 6.

In 1 : 3 complexes, the TMDGA ligand was found to be coordinated *via* three O donor atoms leading to a nona-coordination to the central metal ions. The M–O (O atom of C=O) bond distance was found to be the shortest in Eu^{3+} and longest in La^{3+} and the bond distances follow the order $La^{3+} > Am^{3+} > Cm^{3+} > Eu^{3+} > Lu^{3+}$. Similarly, the C–O (O atom of ether link) bond distances follow the order: $La^{3+} > Am^{3+} > Eu^{3+} > Cm^{3+} > Lu^{3+}$. The M–O (O atom of C=O) bond distance was found to be smaller than the M–O (O atom of ether link) bond distance. Further, in order to test the accuracy of the BP/SVP level of calculation in the prediction of accurate equilibrium geometry, we have optimized the structure of the La^{3+}–$(TMDGA)_3$ complex using the B3LYP/TZVP level of theory and the optimized structure is displayed in Fig. 6. The calculated values are listed in Table 5. The structural parameters obtained using the BP/SVP level of theory are found to be very close to the structural parameters predicted at the B3LYP/TZVP level of theory which justifies the use of the BP86/SVP level of calculation for the geometry optimization. We have also performed the optimization of 1 : 1 and 1 : 2 (M : L) complexes for La^{3+}, Eu^{3+}, Lu^{3+}, Am^{3+} and Cm^{3+} with TMDGA to study the structural and binding evolution of the metal ion–ligand complexes with the successive addition of ligands. The optimized

Table 4 Calculated structural parameters (Å) of the 1 : 3 complexes in the presence of nitrate ions

Metal ion	M–O (O of C=O)	M–O (O of ether)	C=O
La	2.51, 2.46, 2.60, 2.60, 2.52, 2.53	2.74, 2.65, 2.80	1.25, 1.25, 1.25, 1.26, 1.25, 1.24
Eu	2.50, 2.43, 2.51, 2.56, 2.49, 2.44	2.74, 2.54, 2.64	1.25, 1.24, 1.25, 1.25, 1.25, 1.24
Lu	2.24, 2.29, 2.33, 2.38, 2.26, 2.33	2.52, 2.40, 2.58	1,25, 1.25, 1.25, 1.25, 1.25, 1.24
Am	2.45, 2.39, 2.49, 2.52, 2.40, 2.44	2.67, 2.55, 2.81	1.25, 1.25, 1.25, 1.25, 1.25, 1.25
Cm	2.41, 2.36, 2.38, 2.48, 2.38, 2.44	2.63, 2.52, 2.70	1.26, 1.26, 1.25, 1.25, 1.25, 1.25

Table 5 Calculated structural parameters (in Å) of the 1 : 3 complexes without nitrate ions

System	M–O (O of C=O)	M–O (O of ether)	C=O
La	2.53, 2.53, 2.53, 2.53, 2.53, 2.53 (2.53, 2.53, 2.53, 2.53, 2.53, 2.53)	2.72, 2.72, 2.73 (2.75, 2.74, 2.74)	1.26, 1.26, 1.26, 1.26, 1.26, 1.26 (1.25, 1.25, 1.25, 1.25, 1.25, 1.25)
Eu	2.42, 2.43, 2.42, 2.43, 2.41, 2.42	2.65, 2.64, 2.64	1.26, 1.26, 1.26, 1.26, 1.26, 1.26
Lu	2.30, 2.30, 2.31, 2.30, 2.30, 2.30	2.58, 2.54, 2.54	1.26, 1.26, 1.26, 1.26, 1.26, 1.26
Am	2.45, 2.43, 2.41, 2.46, 2.43, 2.42	2.64, 2.65, 2.65	1.26, 1.26, 1.26, 1.26, 1.26, 1.26
Cm	2.43, 2.44, 2.43, 2.43, 2.43, 2.44	2.63, 2.63, 2.63	1.26, 1.26, 1.26, 1.26, 1.26, 1.26

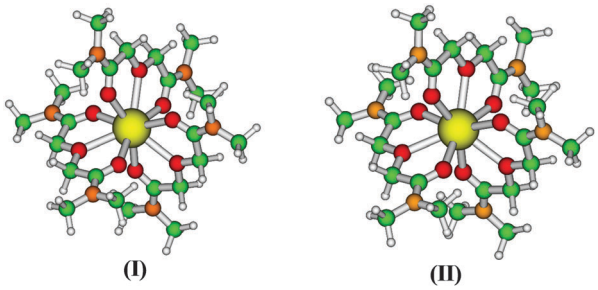

Fig. 6 Optimized minimum energy structures of the metal ion complexes with TMDGA in a 1 : 3 stoichiometry at (I) BP/SVP and (II) B3LYP/TZVP levels of theory. The key is same as in Fig. 1.

structures of M^{3+}–TMDGA complexes with 1 : 1 and 1 : 2 stoichiometries are displayed in Fig. S1 and S2 (ESI†). The calculated structural parameters are listed in Tables S4 and S5 (ESI†). The calculated structural parameters of metal ion–nitrate complexes (1 : 3) are listed in Table 3. All the nitrate ions are found to be coordinated to the metal ion in a bidentate mode *via* O donor atoms leading to six-fold coordination. The M–O distance was found to be 2.49–2.50 Å for La^{3+}, 2.38–2.40 Å for Eu^{3+}, 2.24 Å for Lu^{3+}, 2.37–2.39 Å for Am^{3+} and 2.37–2.39 Å for Cm^{3+} respectively. These values are consistent with the results recently reported by Narbutt *et al.*[13b] for the Eu^{3+} and Am^{3+} complexes of the 2-ethyl-hexyl derivative of DGA (T2EHDGA). The almost same values of the M–O bond distance confirm the similar chemical properties of Eu^{3+}, Am^{3+} and Cm^{3+} and hence makes their individual separation from the nuclear waste a formidable task and therefore, poses a challenge to the experimental and theoretical chemists to develop efficient ligands for their extraction and separation.

We have further complimented the results of B3LYP with MP2 and SCS-MP2 for 1 : 1, 1 : 2 and 1 : 3 stoichiometric complexes of La with TMDGA as for other members of Ln–An, there are no provisions for the calculation at the MP2/SCS-MP2 level of theory due to lack of auxiliary basis sets in TURBOMOLE. The calculated values of the gas phase binding energy for La are presented in Table 6. Recently,[21] it has been reported that the results of SCS-MP2 are very close to the CCSDT results for the aqua lanthanide complexes. In the present case, it is seen that the results obtained for the 1 : 1 complex are very close to the MP2 and SCS-MP2 results (within 2.28% and 3.32%), whereas the MP2 results are within 1.01% of SCS-MP2 results. Further, the BEs calculated for the 1 : 2 and 1 : 3 complexes are within 0.23% and 0.64% of the MP2 values, respectively. Hence, the results obtained at the B3LYP level of theory are reasonable.

Table 6 Values in the parentheses represent the data calculated at B3LYP/TZVP level of theory.Calculated values of the binding energy (kcal/mol) for La^{3+} with TMDGA using different methodologies employing the TZVPP basis set

	Methods		
System	B3LYP	MP2	SCS-MP2
1 : 1	−354.45	−346.54	−343.06
1 : 2	−532.55	−531.30	
1 : 3	−620.31	−624.36	

Stepwise binding energy. The stepwise binding energy in the gas phase is an important parameter to study the complexation behaviour of Ln/An ions with TMDGA. Earlier, time resolved luminescence spectroscopy[30] has been used to study the stepwise stability constant of the Eu^{3+} ion with TODGA, where 1 : 1, 1 : 2 and 1 : 3 species of the Eu^{3+} ion with TODGA were found to be 6.8, 10.1 and 14.3, respectively.

The stepwise complexation of DGA (L) with M^{3+} (M = La, Eu, Lu, Am and Cm) ions can be represented by the reaction,

$$M^{3+} + nL \leftrightarrow M^{3+}\text{–}L_n \ (n = 1\text{–}3) \quad (2)$$

The stepwise complexation is found to be well correlated with the stepwise binding energy,

$$\Delta E_n = E_{M^{3+}\text{–}L_n} - (E_{M^{3+}} + nE_L) \quad (3)$$

as revealed from Fig. 7 and Tables S4–S7 (ESI†). With the successive addition of L, the binding energy was found to increase due to the interaction of the metal ion with a more number of O donor atoms.

Bonding analysis. In order to get more insights into the nature of bonding and interaction of Ln/An with TMDGA,

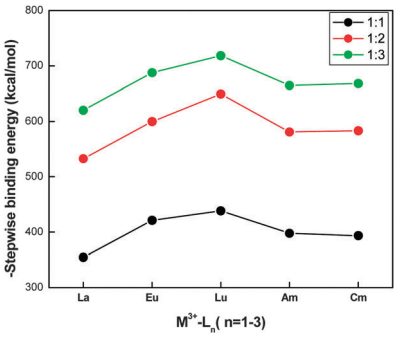

Fig. 7 Calculated stepwise binding energy in the gas phase of the M^{3+}–$(L)_n$ complexes (n = 1–3) at the B3LYP/TZVPP level of theory.

Table 7 Atomic charges and orbital populations (s, p, d, f, g) using natural population analysis on the metal ions for the M^{3+}–$(TMDGA)_3$ complexes (M = La, Eu, Am and Cm) at the B3LYP/TZVPP level of theory

M^{3+}	Charge	*n* (s)	*n* (p)	*n* (d)	*n* (f)	*n* (g)
La	2.27	2.12	5.98	0.605	0.006	0
Eu	1.94	4.14	11.99	10.83	6.07	0.000
Lu	2.01	4.18	11.99	10.80	13.99	0.000
Am	1.96	4.15	11.98	10.74	6.14	0.001
Cm	2.01	4.16	11.98	10.75	7.08	0.001

population analysis, second order interaction energy and topological parameters are discussed in the following sections.

Natural population analysis. Natural population analysis (NPA)[31a] was performed for the M^{3+}–$(TMDGA)_3$ complexes (M = La, Eu, Lu, Am and Cm) to compute the charge on the metal ion and the atomic orbital population. The calculated values of NPA charge and atomic orbital population are listed in Table 7.

The residual charge on the Eu^{3+} ion was found to be smaller (1.94) than Am^{3+} (1.96) and Cm^{3+} (2.01) indicating the highest interaction energy for the Eu^{3+} ion (−687.89 kcal mol^{-1}) compared to Am^{3+} (−664.74 kcal mol^{-1}) and Cm^{3+} ions (−668.19 kcal mol^{-1}). Furthermore, from the NPA analysis, marginal extra orbital contributions to the inner s, d and f sub shells of the metal ions (Eu, Am and Cm) indicate some covalent character. The d sub shells were found to be more diffused than the s, and f sub shells, whereas there is insignificant contribution from *g* sub shells. The f sub shell of Am was found to be more diffused than the others. In the case of the La^{3+} ion, there is almost no extra contribution from f sub shells but a small extra population was found in the s and d sub shells. The bonding analysis for M–$(TMDGA)_3(NO_3)_3$ complexes was also performed and the values are listed in Table S8 (ESI†). The energy of the highest occupied molecular orbital (HOMO) and lowest unoccupied molecular orbital (LUMO) which is known as the frontier molecular orbital and control over the reactivity of the molecular complexation[31b] were also evaluated for M^{3+}–$(TMDGA)_3$ complexes (M = Eu and Am). The HOMO–LUMO energy gap (E_{H-L}) for the trivalent metal ions (Eu = 5.33 eV and Am = 3.97 eV) is found to be high indicating a strong acceptor (*i.e.*, strong acid) and so it can provide a strong electrostatic interaction with strong donor (O atom) based ligands (*i.e.*, strong base), which here is a tridentate chelating TMDGA ligand with a high E_{H-L} value of 6.88 eV. The different selectivities of the metal ions towards the ligands are due to different contributions from the HOMO and LUMO of the respective metal ion–ligand system. In order to calculate the fraction of electrons transferred ($\Delta N = (\chi_M - \chi_L)/\{2(\eta_M + \eta_L)\}$) from the donor TMDGA ligand (L) to the metal ion (M), theoretical values for absolute electronegativity ($\chi = (I + A)/2$) and absolute hardness ($\eta = (I - A)/2$) for Eu and Am metal ions were calculated. Here, $I = -E_{HOMO}$ and $A = -E_{LUMO}$. The theoretical values of absolute electronegativity of Eu and Am metal ions are 34.52 eV and 30.41 eV and absolute hardness are 2.66 eV and 1.98 eV, respectively. This indicates that the Am metal ion is soft acid and the Eu metal ion is hard acid. As per the HSAB principle, hard–hard and soft–soft interactions are preferred among acid–base interactions. The high energy HOMO and large values of hardness (η = 3.44 eV) and electronegativity (χ = 3.15 eV) indicate that TMDGA is a hard base and hence undergoes favorable complexation with the Eu^{3+} ion over the Am^{3+} ion. The favored donor–acceptor interaction is further demonstrated by the large value of ΔN for the Eu^{3+}–$(TMDGA)_3$ complex (2.56) over the Am^{3+}–$(TMDGA)_3$ complex (2.51) and hence also supports their extraction behaviors.

Atom in molecule (AIM) topological parameters. The bond critical point (BCP) which is measured from topological parameters such as electron density (ρ) and the Laplacian of electron density ($\nabla^2\rho$) can be used to describe the nature of bonding in a molecule[32] and is calculated here using the AIM theory of ADF package[33] at B3LYP/TZ2P level of theory. The bond strength is attributed to the electron density at the BCP (ρ) and a large electron density leads to a strong bond. Similarly, a bond is said to be covalent if $\nabla^2\rho < 0$ and closed-shell bonding if $\nabla^2\rho > 0$. The ellipticity (ε) of the bond measures the extent to which density is preferentially accumulated in a given plane containing the bond path.

The calculated values of various topological parameters ρ, $\nabla^2\rho$ and ellipticity (ε) for M^{3+}–$(TMDGA)_3$ complexes (M = Eu and Am) are tabulated in Table 8 (details are summarized in Table S9, ESI†) and BCPs are shown in Fig. 8.

From the figure, the presence of 9 BCPs from 9 donor O atoms to centrally located metal ions is clearly visible. Further, from the table it is seen that the average value of ρ is positive but small and is found to be slightly higher for the Am^{3+} ion (0.048) than the Eu^{3+} ion (0.042). Similarly, the average value of $\nabla^2\rho$ was found to be positive indicating the closed shell interaction between the donor atoms and acceptor metal ions and the value was found to be little higher for the Am^{3+} ion (0.207) compared to the Eu^{3+} ion (0.182) indicating a more ionic character for the Am^{3+} ion than the Eu^{3+} ion. Moreover, these interactions are stronger than the hydrogen bond as the values of electron density ρ (0.042–0.048 e au^{-3}) and $\nabla^2\rho$ (0.182–0.207 e au^{-5}) are higher than that of hydrogen (0.0002–0.035 e au^{-3} and

Table 8 Average electron density and Laplacian of electron density and ellipticity for the M^{3+}–$(TMDGA)_3$ and aqua complexes at the B3LYP/TZ2P level of theory using Bader's AIM calculations

Complex	BCP	Avg.ρ	Avg. $\nabla^2\rho$	Avg.ε [$\varepsilon = (\lambda_1/\lambda_2) - 1$]
TMDGA				
La	La–O	0.037	0.144	0.016
Eu	Eu—O	0.041	0.189	0.196
Lu	Lu–O	0.045	0.200	0.014
Am	Am–O	0.046	0.214	0.517
Cm	Cm–O	0.046	0.200	0.018
H_2O				
La	La–O	0.033	0.132	0.148
Eu	Eu–O	0.036	0.156	0.105
Lu	Lu–O	0.041	0.186	0.096
Am	Am–O	0.039	0.167	0.127
Cm	Cm–O	0.042	0.182	0.120

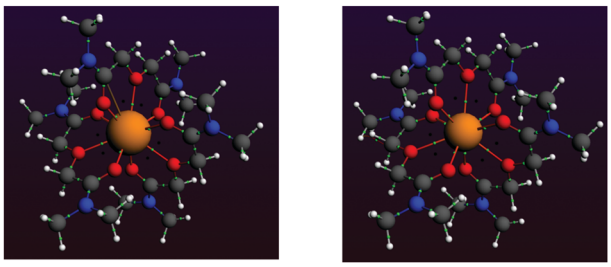

Fig. 8 Calculated BCP from O atoms to the metal ion of the $Eu^{3+}(TMDGA)_3$ and $Am^{3+}(TMDGA)_3$ complexes at B3LYP/TZ2P level of theory.

0.024–0.139 e au^{-5}, respectively). The average value of ellipticity is found to be quite small (0.0.025 and 0.048 for Eu^{3+} and Am^{3+} ions, respectively) indicating small covalency but it is smaller in Am than Eu.

Further, Laplacian density has also been calculated for the aqua ions and is presented in Table 8. Here, also the average electron density and Laplacian of electron density for Am are found to be higher than the Eu ion as observed with the TMDGA ligands and thus indicating a higher ionic character for Am over Eu. The average electron density and Laplacian of electron density are found to be higher with TMDGA ligands over aqua ligands. The higher ionic character of Am over Eu predicted from Laplacian density is in contrast to the other reports[12b,34] where higher covalency has been shown for actinides towards O donors over N donors which are considered to be softer than O atoms. In the present case, the higher covalency for actinides has not been observed which seems to be apparently obvious.

Second order stabilization energy. The second order interaction energy, $E_{ij}^{(2)}$ which is a measure of the strength of coordinated interaction can be used to predict the selectivity of metal ions (acceptor) towards ligands (donor). The value of $E_{ij}^{(2)}$ for Eu^{3+} and Am^{3+} complexes with TMDGA is evaluated using the NBO5.0[35] module of ADF package[33] at B3LYP/TZ2P level of theory. The stability of a metal ion complex is indicated by a large value of $E_{ij}^{(2)}$. The stabilization energy $E_{ij}^{(2)}$ between the donor NBO (i) and the acceptor NBO (j) is calculated using the following relation:

$$E_{ij}^{(2)} = q_i \times F_{(ij)}^2/(\varepsilon_i - \varepsilon_j) \quad (4)$$

where q_i is the donor orbital occupancy, ε_i and ε_j are diagonal elements (orbital energies), and $F_{(ij)}^2$ is the off-diagonal NBO Fock matrix element. The strength of charge transfer interaction between the NBO donor and the NBO acceptor dictates the value of $E_{ij}^{(2)}$. A high stabilization energy is obtained for a strong donor–acceptor interaction The details of the calculations of $E_{ij}^{(2)}$ are presented in Table S10, ESI.† Nine lone pairs of oxygen atoms, LP (O), act as the NBO donor and the anti bonding vacant orbital of metal ions (M = Eu and Am) as the NBO acceptor, LP*(M = Eu and Am). The average stabilization energy from the nine lone pairs of O atoms with TMDGA (3 units) ligand is found to be higher for the Eu^{3+} ion (2.47 kcal mol^{-1}) compared to the Am^{3+} ion (1.58 kcal mol^{-1}), thus confirming the selectivity *i.e.* the Eu^{3+} ion which has a higher gas phase binding energy (−687.89 kcal mol^{-1}) shows the highest stabilization energy and Am^{3+} shows a smaller second order stabilization energy with a smaller gas phase binding energy (−664.74 kcal mol^{-1}).

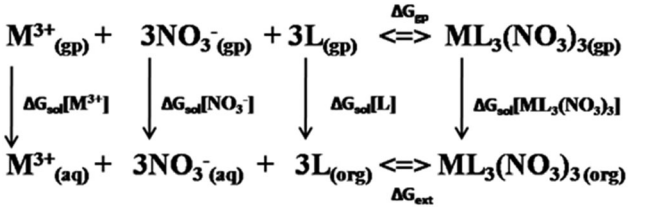

Scheme 1 Thermodynamic cycle for the extraction of metal ions where the metal ions and nitrate ions are considered to be separate solvated species.

Free energy of extraction. The extraction of metal ions from the aqueous phase to the organic phase using the TMDGA ligand can be predicted using free energy of extraction, ΔG_{ext}. The free energy of extraction, ΔG_{ext}, data (computed using the thermodynamic cycle of Scheme 1, where the metal ions were considered to be isolated species in aqueous solution as mentioned in eqn (1)) for the transfer of metal ions (La^{3+}, Eu^{3+}, Lu^{3+}, Am^{3+} and Cm^{3+}) from aqueous to *n*-dodecane organic phases with the TMDGA ligand using eqn (1) for 1 : 3 stoichiometric complexation reactions are listed in Table 9.

Scheme 1 suggests that the solvation energy of metal ions plays a very decisive role. Hence, the solvation of metal ions has been considered using two different solvation approaches: namely, explicit monomer water and cluster water solvation models. The details are presented below.

Explicit solvation approach using monomer water of Scheme 1. This explicit solvation scheme is based on the solvation model of Dolg *et al.*[36] The metal ions with 9 water units in the first solvation shell were solvated in the COSMO phase as

$$M^+_{(gas)} + 9H_2O_{(aq)} \rightarrow M^+(H_2O)_{9(aq)} \quad (5)$$

whereas the solvation free energy of nitrate ions was taken from earlier published data.[37] The computed value of free energy of extraction, ΔG_{ext}, for the transfer of metal ions from the aqueous to the dodecane phase using explicit solvation of bare metal ions according to Scheme 1 is displayed in Table 9. The computed value of ΔG_{ext} was found to be exergonic indicating that TMDGA ligands are able to extract the metal ions from the

Table 9 Calculated values of the thermodynamic parameters (kcal mol^{-1}) for the extraction of different hydrated Ln–An complexes in the presence of nitrate anions with TMDGA at the B3LYP/TZVPP level of calculation (T = 298.15 K; Scheme 1, monomer water, COSMO)

M^{3+}	$\Delta G_{(gp)}$	$\Delta G_{sol(M)}$	$\Delta G_{sol(NO_3)}$	$\Delta G_{sol(ML_3(NO_3)_3)}$	ΔG_{ext}	$\Delta\Delta G_{sol}$
La	−901.99	−711.37	−54.23	−14.77	−22.25	879.74
Eu	−975.20	−775.55	—	−15.62	−32.12	943.08
Lu	−1011.09	−813.34	—	−16.05	−30.64	980.44
Am	−947.43	−755.00	—	−16.43	−25.71	921.72
Cm	−948.51	−756.81	—	−15.78	−24.33	924.18

aqueous phase to the dodecane phase. The free energy of extraction was found to be highest for the Eu^{3+} ion and lowest for the La^{3+} ion and the values for Lu^{3+}, Am^{3+} and Cm^{3+} are in between. The calculated preferential selectivity follows the order $Eu^{3+} > Lu^{3+} > Am^{3+} > Cm^{3+} > La^{3+}$, whereas the distribution ratio in the solvent extraction experiments (Table 1) follows the trend $Lu^{3+} > Eu^{3+} > Cm^{3+} > Am^{3+} > La^{3+}$ and similar trends were also reported in the literature under different experimental conditions.[6d,38]

Though the calculated selectivity order in solution phase does not exactly match the experimental trend but the gas phase calculated value follows the experimental trend nicely. The calculated solution phase ΔG_{ext}, predicted lower extraction of Lu^{3+} as compared to Eu^{3+}. The calculated values of ΔG_{gp} and $\Delta\Delta G_{sol}$ for all the ions are also presented in Table 9 in order to understand the effect of solvent on the free energy. From the values it is observed that the selectivity predicted using gas phase free energy changes after inclusion of $\Delta\Delta G_{sol}$ arising due to the solvent effect. Also, the value has been reduced drastically due to dielectric screening of the solvent. So solvent plays an important role in the thermodynamic selectivity. In view of that in the next section the free energy of solvation for the metal ions has been calculated.

Water cluster solvation approach of Scheme 1. In this scheme, the cluster solvation approach of Goddard *et al.*[39] was used where within a cluster of water molecules, the metal ion is submerged as:

$$M^{+}_{(gas)} + (H_2O)_{9(aq)} \rightarrow M^{+}(H_2O)_{9(aq)} \quad (6)$$

Here, the cluster of water consisting of 9 water units was used for the optimization of the structures followed by the evaluation of total energy. The default COSMO radii of atoms were considered for the solvation effect calculation. The computed value of free energy of extraction, ΔG_{ext}, for the transfer of metal ions from the aqueous to the dodecane phase using explicit solvation of bare metal ions according to Scheme 1 is listed in Table 10.

The computed value of ΔG_{ext} was found to be positive and hence indicating that the extraction of metal ions using the cluster solvation model is not workable. A point to be mentioned is that the standard state entropy correction was made in the evaluation of free energy of solvation of metal ions by adopting the reported methodology of Goddard *et al.*[39] and Shamov *et al.*[40] Further, we have performed the free energy calculations in the absence of NO_3^- ions. In the absence of NO_3^- ions we were unable to predict the negative free energy of extraction (see Table S5, ESI†). In Scheme 1, the metal was considered to be an isolated hydrated species. It is interesting to study when the metal and nitrate ions exist as an ion pair in aqueous solution as mentioned in eqn (6). In the presence of nitrate ions, the hydrated metal ions prefer to coordinate with the nitrate ions which act as bidentate ligands in both the gas and aqueous phases. Consideration of this ion pair model can be justified by the following stability analysis of the hydrated metal ions and hydrated metal–nitrate species. The trivalent metal ion is shown to be nona-hydrated. Now, the stability of this hydrated cluster during complexation with nitrate ions can be checked using the free energy of the following complexation reaction:

$$M^{+}(H_2O)_{9(gas)} + 3NO_3^{-}{}_{(gas)} \rightarrow M(NO_3)_3(H_2O)_{5(gas)} + 4H_2O \quad (7)$$

The calculated value of free energy change (Table S11, ESI†) for the above reaction is found to be negative which indicates the possibility of forming the hydrated nitrate ion pair species. According to the Gibbs free energy value, the metal nitrate hydrates are more stable than the metal hydrates indicating that nitrate ions have stronger coordination ability than water molecules. Further, recently, a hydrated nitrate ion pair has been tested as a model for free energy calculations.[41] Hence, the free energy of extraction was then further computed using the thermodynamic cycle of Scheme 2. The solvation of metal nitrates has been considered using two different solvation approaches: namely, explicit monomer and cluster water solvation models as follows.

Explicit solvation approach using monomer water of Scheme 2. This solvation approach is based on the explicit solvation model using monomer water. The gas phase metal nitrate with first solvation sphere water molecules (assuming 5 water units) was solvated as

$$M(NO_3)_{3(gas)} + 5H_2O_{(aq)} \rightarrow M(NO_3)_3(H_2O)_{5(aq)} \quad (8)$$

The computed value of free energy of extraction, ΔG_{ext}, for the transfer of metal ions from the aqueous to the dodecane phase using the explicit solvation of cation–anion ion pair model according to Scheme 2 is listed in Table S12 (ESI†).

Table 10 Calculated value of the thermodynamic parameters (kcal mol^{-1}) for the extraction of different hydrated Ln–An complexes in the presence of nitrate anions with TMDGA at the B3LYP/TZVPP level of calculation (T = 298.15 K; Scheme 1, cluster water, COSMO)

M^{3+}	$\Delta G_{(gp)}$	$\Delta G_{sol(M)}$	$\Delta G_{sol(NO_3)}$	$\Delta G_{sol(ML_3(NO_3)_3)}$	ΔG_{ext}	$\Delta\Delta G_{sol}$
La	−901.99	−754.01	−54.23	−14.77	20.38	922.38
Eu	−975.20	−818.19	—	−15.62	10.51	983.90
Lu	−1011.09	−855.98	—	−16.05	11.99	1023.08
Am	−947.43	−797.64	—	−16.43	16.92	964.36
Cm	−948.51	−799.45	—	−15.78	18.31	966.82

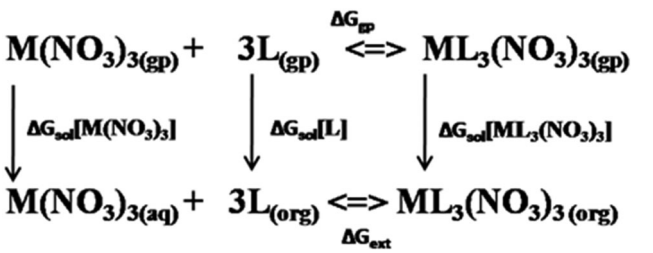

Scheme 2 Thermodynamic cycle for the extraction of the metal ion where the metal ion is considered to be in hydrated nitrate form.

The calculated value of ΔG_{gp} is found to be negative only for the La^{3+} ion and positive for other metal ions. The contribution of a high positive value of $\Delta\Delta G_{sol}$ makes the overall extraction free energy, ΔG_{ext} positive suggesting that the extraction is unfavourable. Hence, the extraction of the hydrated metal nitrate using the explicit monomer water solvation model is not workable due to positive free energy of extraction.

Water cluster solvation approach of Scheme 2. In this scheme, the cluster of water molecules was considered for solvation of the metal nitrate. The metal nitrate is immersed in the cluster of water molecules as described below:

$$M(NO_3)_{3(gas)} + (H_2O)_{5(aq)} \rightarrow M(NO_3)_3(H_2O)_{5(aq)} \quad (9)$$

The computed value of free energy of extraction, ΔG_{ext}, for the transfer of metal ions from the aqueous to the dodecane phase using explicit solvation of metal nitrate according to Scheme 2 is listed in Table S13 (ESI†). The computed value of ΔG_{ext} was found to be positive and more positive compared to monomer water model due to a more positive contribution of $\Delta\Delta G_{sol}$ and hence suggesting that the extraction of metal ions using cluster solvation model of Scheme 2 is thermodynamically unfavourable. From the present study, it has been observed that the calculated free energy of extraction employing the ion pair model fails for both the monomer and cluster water models and hence cannot be used to predict the experimental metal ion selectivity. Though Scheme 1 using the monomer water model is exergonic it fails to captures the correct trend of Ln/An extraction using TODGA in the aqueous–dodecane biphasic system. This might be due to non-consideration of dispersion of a large molecular system. Therefore, we have further performed the dispersion correction following the Grimme's DFT-D3[42] methodology as implemented in Turbomole for the calculation of free energy for La, Lu and Eu only as no parameterization is available for Am and Cm.

The calculated results using DFT-D3 for the monomer and cluster water models are presented in Tables 11 and 12 respectively.

From Table 11, it is seen that the calculated value of metal ion solvation energy was found to be increased after dispersion correction. The solvation energy of the free ligand and the metal–nitrate–ligand complexes was observed to be unchanged. Also all the other interaction energy parameters were seen to be increased due to dispersion correction. The gas phase metal–nitrate–ligand complexation free energy was found to be increased substantially and was found to be highest for the Lu ion due to a smaller size. After dispersion correction, the free energy of extraction for the metal ions was seen to follow the order: Lu > Eu > La, which was also observed in the solvent extraction experiments.

Table 11 Calculated values of the thermodynamic parameters (kcal mol^{-1}) for the extraction of different hydrated Ln–An complexes in the presence of nitrate anions with TMDGA at the B3LYP-D3/TZVPP level of calculation (T = 298.15 K; Scheme 1, monomer water, COSMO)

M^{3+}	$\Delta G_{(gp)}$	$\Delta G_{sol(M)}$	$\Delta G_{sol(NO_3)}$	$\Delta G_{sol(ML_3(NO_3)_3)}$	ΔG_{ext}	$\Delta\Delta G_{sol}$
La	−955.13	−770.26	−54.23	−14.77	−16.52	938.61
Eu	−1028.57	−842.49	—	−15.66	−18.60	1009.96
Lu	−1068.91	−877.56	—	−16.04	−24.26	1044.64

Table 12 Calculated values of the thermodynamic parameters (kcal mol^{-1}) for the extraction of different hydrated Ln–An complexes in the presence of nitrate anions with TMDGA at the B3LYP-D3/TZVPP level of calculation (T = 298.15 K; Scheme 1, cluster water, COSMO)

M^{3+}	$\Delta G_{(gp)}$	$\Delta G_{sol(M)}$	$\Delta G_{sol(ML_3(NO_3)_3)}$	ΔG_{ext}	$\Delta\Delta G_{sol}$
La	−955.13	−755.24	−14.77	−31.54	923.59
Eu	−1028.57	−827.47	−15.66	−33.62	994.94
Lu	−1068.91	−862.54	−16.04	−39.28	1029.62

The cluster model (Table 12) also predicts the same trend as observed in the experiments. Both the monomer and cluster water models correctly predict the experimental trend for lanthanides. Since, no dispersion correction scheme is available for Am and Cm, the selectivity trend for Ln and An cannot be predicted. Nevertheless, it is anticipated that the dispersion corrected scheme in conjunction with COSMO might work with actinides also which in future can be checked once the B3LYP-D3 parameterization for Am and Cm becomes available.

COSMO *versus* COSMO-RS

In the earlier section, it has been observed that the COSMO solvation model does not work at the B3LYP level without dispersion which is a purely dielectric continuum model. Hence, it will be worthwhile to check whether the failure is due to the limitation of the dielectric continuum model which does not account for the structure of the solvents. In view of that, a self-consistent variant of COSMO-RS[43] that incorporates the structure of the solvents by incorporating the surface charge densities through well defined sigma potentials has been used. The calculation has been performed using the D-COSMO-RS[44] module of Turbomole. The required sigma potential for water has been taken from the Turbomole library, whereas for dodecane, the sigma potential of hexane available in the library has been used. The calculated values of thermodynamic free energy using the DCOSMO-RS method at the B3LYP level of theory using the monomer water model of Scheme 1 are presented in Table S14 (ESI†). The free energy of solvation of the metal ions was seen to be reduced compared to the value obtained from the COSMO model, whereas the free energy of solvation for the free ligand and the metal–ligand complexes were seen to be increased. The calculated free energy of extraction follows the order: Eu > Lu > Am > Cm > La, whereas the experimental order is: Lu > Eu > Cm > Am > La. The calculated results cannot predict the correct experimental trends as also observed in the case of the COSMO model. Next, free energy of extraction for the metal ions was evaluated using the cluster water model of Scheme 1 and the values are presented in Table S15 (ESI†). The cluster model even fails to capture the exergonic nature of the metal ion extraction and hence might not be suitable for the selectivity calculation.

Furthermore, the free energy of extraction was calculated using DFT-D3 in conjunction with the COSMO-RS model for

Table 13 Calculated values of the thermodynamic parameters (kcal mol^{-1}) for the extraction of Ln–An complexes in the presence of nitrate anions with TMDGA at the B3LYP-D3/TZVPP level of calculation (T = 298.15 K; Scheme 1, monomer water, COSMO-RS)

M^{3+}	$\Delta G_{(gp)}$	$\Delta G_{sol(M)}$	$\Delta G_{sol(L)}$	$\Delta G_{sol(ML_3(NO_3)_3)}$	ΔG_{ext}	$\Delta\Delta G_{sol}$
La	−955.13	−753.43	−17.10	−38.26	−25.96	929.16
Eu	−1028.57	−822.79		−36.26	−28.04	1000.53
Lu	−1068.91	−860.73		−38.57	−32.74	1036.16

both monomer and cluster solvation models of Scheme 1. The calculated values using the monomer water model are presented in Table 13. The free energy of solvation for metal ions was seen to be decreased, whereas the free energy of solvation for the free ligand and metal–ligand complexes were seen to be increased. From the calculated values it is seen that the metal ion selectivity follows the same order as observed using the DFT-D3 and COSMO combination *i.e.* Lu > Eu > La, which was also observed in the solvent extraction experiments. In the case of the cluster water model, the free energy of solvation for metal ions, free ligand and metal–ligand complexes was found to be increased compared to DFT-D3 and COSMO combination (Table S16, ESI†). In the case of the cluster water model also, the metal ion selectivity follows the same order as with the DFT-D3 and COSMO-RS for monomer water model combination *i.e.* Lu > Eu > La as observed in the solvent extraction experiments. It is worth noting that the TMDGA may have multiple conformers. In view of that conformational sampling was performed using the COSMOconf algorithm. Details are given in the ESI.† (Fig. S1 and Table S17)

Conclusions

The present DFT based study demonstrates the structure, bonding, and energetic and thermodynamic parameters of lanthanide and actinide metal ions extracted with diglycolamide in the gas phase and the solvent phase. The calculated structures obtained at BP/SVP level of calculation are found to be in close agreement with the structures obtained at B3LYP/TZVP level of theory and with the X-ray data. The presence of nitrate ions and water molecules is found to be indispensable for modeling the extraction of lanthanide and actinide ions from the aqueous phase to the dodecane organic solvent phase using the COSMO solvation approach. The computed value of ΔG_{ext} using the thermodynamic cycle was found to be exergonic indicating that TMDGA ligands are able to extract the metal ions from the aqueous phase to the dodecane phase. The calculated preferential selectivity follows the order Eu^{3+} > Lu^{3+} > Am^{3+} > Cm^{3+} > La^{3+}, whereas the distribution ratio in the solvent extraction experiments (Table 1) follows the trend Lu^{3+} > Eu^{3+} > Cm^{3+} > Am^{3+} > La^{3+}. Though the calculated selectivity order in the solution phase does not exactly match the experimental trend the gas phase calculated value follows the experimental trend nicely. The calculated solution phase ΔG_{ext} predicted lower extraction of Lu^{3+} as compared to Eu^{3+}. This might be due to non-consideration of dispersion of a large molecular system. After dispersion correction (DFT-D3), the free energy of extraction for the metal ions was seen to follow the order: Lu > Eu > La, which was also observed in the solvent extraction experiments. Since, no dispersion correction scheme is available for Am and Cm, the selectivity trend for Ln and An cannot be predicted. Nevertheless, it is anticipated that the dispersion corrected scheme in conjunction with COSMO might work with actinides also. It is worthwhile to mention that both COSMO and COSMO-RS work excellently when they are combined with the more accurate DFT-D3 level of calculation for the prediction of the selectivity trend (Lu > Eu > La). Bonding analyses were performed to study the ionic and covalent nature of the interaction of metal ions with the TMDGA ligand. The present results successfully capture the experimental selectivity order taking into account the complete molecular stoichiometry, anions and experimentally used organic solvents which were not considered by previously reported DFT studies on this system. In the present case, a lower analogue of TODGA (TMDGA) has been used to simulate the experimental selectivity to keep the computation tractable. Nevertheless, if the dispersion correction is performed with the TODGA molecule, only the contribution from the dispersion will be more due to the large molecular size of TODGA compared to TMDGA but the selectivity trend will remain the same as the extent of interaction of the metal ions towards TODGA will be similar to that observed for TMDGA. The results obatined from the present study will further help in the understanding of Ln/An complexation with DGA and hence in the improved design of ligands for Ln/An extraction from high level liquid waste.

Acknowledgements

Computer Division, BARC is acknowledged for providing the Anupam supercomputing facility. We sincerely acknowledge Dr A. Goswami, Ex-Head, RCD, Dr S. B. Roy, Associate Director, ChEG and Mr K. T. Shenoy, Head, ChED for continuous encouragement.

References

1 (*a*) J. N. Mathur, M. S. Murali and K. L. Nash, *Solvent Extr. Ion Exch.*, 2008, **19**, 357–390; (*b*) S. A. Ansari, P. N. Pathak, P. K. Mohapatra and V. K. Manchanda, *Sep. Purif. Rev.*, 2011, **40**, 43–76.

2 (*a*) W. W. Schulz and E. P. Horwitz, *Sep. Sci. Technol.*, 1988, **23**, 1191–1210; (*b*) A. Ramanujam, P. S. Dhami, V. Gopalakrishnan, N. L. Dudwadkar, R. R. Chitnis and J. N. Mathur, *Sep. Sci. Technol.*, 1999, **34**, 1717–1728; (*c*) B. J. Mincher, N. C. Schmitt and M. E. Case, *Solvent Extr. Ion Exch.*, 2011, **29**, 247–259; (*d*) E. P. Horwitz, A. C. Muscatello, D. G. Kalina and L. Kaplan, *Sep. Sci. Technol.*, 1981, **16**, 417–437; (*e*) B. J. Mincher, *Solvent Extr. Ion Exch.*, 1989, **7**, 645–654.

3 (*a*) X. Liu, J. Liang and J. Xu, *Solvent Extr. Ion Exch.*, 2004, **22**, 163–173; (*b*) C. Jing, W. Jianchen and S. Chongli, *Tsinghua Sci. Technol.*, 2001, **6**, 180–184.
4 S. Tachimori and H. Nakamura, *J. Nucl. Sci. Technol.*, 1982, **19**, 326–333.
5 (*a*) H. B. Yang, E. H. Lee, J. K. Lim, D. Y. Chung and K. W. Kim, *J. Radioanal. Nucl. Chem.*, 2009, **280**, 495–502; (*b*) D. Serrano-Purroy, P. Baron, B. Christiansen, R. Malmbeck, C. Sorel and J. P. Glatz, *Radiochim. Acta*, 2005, **93**, 351–355; (*c*) G. Modolo, H. Vijgen, D. Serrano-Purroy, B. Christiansen, R. Malmbeck, C. Sorel and P. Baron, *Sep. Sci. Technol.*, 2007, **42**, 439–452; (*d*) L. B. Kumbhare, D. R. Prabhu, G. R. Mahajan, S. Sriram, V. K. Manchanda and L. P. Badheka, *Nucl. Technol.*, 2002, **139**, 253–262.
6 (*a*) R. B. Gujar, S. A. Ansari, D. R. Prabhu, P. N. Pathak, A. Sengupta, S. K. Thulasidas, P. K. Mohapatra and V. K. Manchanda, *Solvent Extr. Ion Exch.*, 2012, **30**, 156–170; (*b*) D. Magnusson, B. Christiansen, J. P. Glatz, R. Malmbeck, G. Modolo, D. Serrano-Purroy and C. Sorel, *Solvent Extr. Ion Exch.*, 2009, **27**, 26–35; (*c*) S. A. Ansari, P. N. Pathak, P. K. Mohapatra and V. K. Manchanda, *Chem. Rev.*, 2012, **112**, 1751–1772; (*d*) Y. Sasaki, Y. Sugo, S. Suzuki and S. Tachimori, *Solvent Extr. Ion Exch.*, 2001, **19**, 91–103.
7 (*a*) S. Panja, P. K. Mohapatra, S. C. Tripathi and V. K. Manchanda, *J. Hazard. Mater.*, 2011, **188**, 281–287; (*b*) J. N. Sharma, R. Ruhela, K. N. Harindaran, S. L. Mishra, S. K. Tangri and A. K. Suri, *J. Radioanal. Nucl. Chem.*, 2008, **278**, 173–177.
8 J. Ravi, A. S. Suneesh, T. Prathibha, K. A. Venkatesan, M. P. Antony, T. G. Srinivasan and P. R. Vasudeva Rao, *Solvent Extr. Ion Exch.*, 2011, **29**, 86–105.
9 S. Kannan, M. A. Moody, C. L. Barnes and P. B. Duval, *Inorg. Chem.*, 2008, **47**, 4691–4695.
10 (*a*) G. Tian, J. Xu and L. Rao, *Angew. Chem., Int. Ed.*, 2005, **44**, 6200–6203; (*b*) S. D. Reilly, A. J. Gaunt, B. L. Scott, G. Modolo, M. Iqbal, W. Verboom and M. J. Sarsfield, *Chem. Commun.*, 2012, **48**, 9732–9734.
11 (*a*) H. Narita, T. Yaita, S. Tachimori, Proceedings of International Solvent Extraction Conference 1999 (ISEC99), pp. 693–696; (*b*) M. R. Antonio, D. R. McAlister and E. P. Horwitz, *Dalton Trans.*, 2015, **44**, 515–521.
12 (*a*) X. Cao, D. Heidelberg, G. Ciupka and M. Dolg, *Inorg. Chem.*, 2010, **49**, 10307–10315; (*b*) L. E. Roy, N. J. Bridges and L. R. Martin, *Dalton Trans.*, 2013, **42**, 2636–2642; (*c*) J. M. Keith and E. R. Batista, *Inorg. Chem.*, 2012, **51**, 13–15.
13 (*a*) C.-Z. Wang, J.-H. Lan, Q.-Y. Wu, Y.-L. Zhao, X.-K. Wang, Z.-F. Chai and W.-Q. Shi, *Dalton Trans.*, 2014, **43**, 8713–8720; (*b*) J. Narbutt, A. Wodyński and M. Pecul, *Dalton Trans.*, 2015, **44**, 2657.
14 (*a*) A. D. Becke, *Phys. Rev. A: At., Mol., Opt. Phys.*, 1988, **38**, 3098–3100; (*b*) J. P. Perdew, *Phys. Rev. B: Condens. Matter Mater. Phys.*, 1986, **33**, 8822–8824.
15 K. Eichkorn, F. Weigend, O. Treutler and R. Ahlrichs, *Theor. Chem. Acc.*, 1997, **97**, 119.
16 (*a*) R. Ahlrichs, M. Baer, M. Haeser, H. Horn and C. Koelmel, *Chem. Phys. Lett.*, 1989, **162**, 165–169; (*b*) O. Treutler and R. Ahlrichs, *J. Chem. Phys.*, 1995, **102**, 346–354; (*c*) TURBOMOLE V6.6 a development of University of Karlsruhe and Forschungszentrum Karlsruhe GmbH, 1989–2007, TURBOMOLE GmbH, since 2007; available from http://www.turbomole.com.
17 (*a*) M. Dolg, H. Stoll, A. Savin and H. Preuss, *Theor. Chim. Acta*, 1989, **75**, 173; (*b*) M. Dolg, H. Stoll and H. Preuss, *Theor. Chim. Acta*, 1993, **85**, 441.
18 M. Dolg, H. Stoll and H. Preuss, *J. Chem. Phys.*, 1989, **90**, 1730.
19 X. Cao and M. Dolg, *J. Chem. Phys.*, 2001, **115**, 7348; X. Cao and M. Dolg, *THEOCHEM*, 2002, **581**, 139.
20 (*a*) W. Kuechle, M. Dolg, H. Stoll and H. Preuss, *J. Chem. Phys.*, 1994, **100**, 7535; (*b*) X. Cao, M. Dolg and H. Stoll, *J. Chem. Phys.*, 2003, **118**, 487*cf.* also X. Cao and M. Dolg, *THEOCHEM*, 2004, **673**, 203.
21 J. Zhang, N. Heinz and M. Dolg, *Inorg. Chem.*, 2014, **53**, 7700–7708.
22 F. Neese, *Coord. Chem. Rev.*, 2009, **253**, 526–556.
23 (*a*) A. D. Becke, *J. Chem. Phys.*, 1993, **98**, 5648–5652; (*b*) C. Lee, W. Yang and R. G. Parr, *Phys. Rev. B: Condens. Matter Mater. Phys.*, 1988, **37**, 785–789.
24 (*a*) F. Weigend and R. Ahlrichs, *Phys. Chem. Chem. Phys.*, 2005, **7**, 3297; (*b*) A. Schäfer, C. Huber and R. Ahlrichs, *J. Chem. Phys.*, 1994, **100**, 5829.
25 A. Klamt, *J. Phys. Chem.*, 1995, **99**, 2224–2235.
26 (*a*) Y. Sasaki, Y. Sugo, S. Suzuki and S. Tachimori, *Solvent Extr. Ion Exch.*, 2001, **19**(1), 91–103; (*b*) Z. X. Zhu, Y. Sasaki, H. Suzuki, S. Suzuki and T. Kimura, *Anal. Chim. Acta*, 2004, **527**, 163–168.
27 B. Machura, A. S. Witlicka, J. Palion and R. Kruszynski, *Struct. Chem.*, 2013, **24**, 89–96.
28 (*a*) S. Hazra, S. Naskar, D. Mishra, S. I. Gorelsky, H. M. Figgie, W. S. Sheldrick and S. K. Chattopadhyay, *Dalton Trans.*, 2007, 4143–4148; (*b*) A. C. Behrle, C. L. Barnes, N. Kaltsoyannis and J. R. Walensky, *Inorg. Chem.*, 2013, **52**, 10623–10631.
29 B. Eriksson and L. O. Larsson, *J. Chem. Soc., Chem. Commun.*, 1978, 616–617.
30 (*a*) P. N. Pathak, S. A. Ansari, S. V. Godbole, A. R. Dhobale and V. K. Manchanda, *Spectrochim. Acta, Part A*, 2009, **73**, 348–352.
31 (*a*) A. E. Reed, R. B. Weinstock and F. Weinhold, *J. Chem. Phys.*, 1985, **83**, 735–746; (*b*) K. Fukui, *Angew. Chem., Int. Ed. Engl.*, 1982, **21**, 801–809.
32 C. F. Matta and R. J. Boyd, *An introduction to the Quantum Theory of Atoms in Molecules*, Willey-VCH Verlag GmbH, Weinheim, 2007, pp. 1–34.
33 (*a*) ADF2013, SCM, Theoretical Chemistry, Vrije Universiteit, Amsterdam, The Netherlands, http://www.scm.com; (*b*) G. te Velde, F. M. Bickelhaupt, E. J. Baerends, C. Fonseca, S. J. A. van Gisbergen, J. G. Snijders and T. Ziegler, *J. Comput. Chem.*, 2001, **22**, 931–967.
34 C. Adam, P. Kaden, B. B. Beele, U. Müllich, S. Trumm, A. Geist, P. J. Panaka and M. A. Denecke, *Dalton Trans.*, 2013, **42**, 14068.

35 E. D. Glendening, O. K. Badenhoop, A. E. Reed, J. E. Carpenter, J. A. Bohmann, C. M. Morales and F. Weinhold, *NBO 5.0*, TCI, University of Wisconsin, Madison, WI, 2001.
36 J. Ciupka, X. Cao-Dolg, J. Wiebke and M. Dolg, *Phys. Chem. Chem. Phys.*, 2010, **12**, 13215–13223.
37 A. Boda and S. M. Ali, *J. Phys. Chem. A*, 2012, **116**, 8615.
38 (*a*) R. B. Gujar, S. A. Ansari, P. K. Mohapatra and V. K. Manchanda, *Solvent Extr. Ion Exch.*, 2010, **28**, 350–366; (*b*) E. A. Mowafy and H. F. Aly, *Solvent Extr. Ion Exch.*, 2007, **25**, 205–224.
39 V. S. Bryantsev, M. S. Diallo and W. A. Goddard III, *J. Phys. Chem. B*, 2008, **112**, 9709–9719.
40 G. A. Shamov and G. Schreckenbach, *J. Phys. Chem. A*, 2005, **109**, 10961–10974.
41 C. Wang, J. Lan, Y. Zhao, Z. Chai, Y. Wei and W. Shi, *Inorg. Chem.*, 2013, **52**, 196–203.
42 S. Grimme, J. Antony, S. Ehrlich and H. Krieg, *J. Chem. Phys.*, 2010, **132**, 154104.
43 A. Klamt, *Wiley Interdiscip. Rev.: Comput. Mol. Sci.*, 2011, **1**, 699–709; F. Eckert and A. Klamt, *AIChE J.*, 2002, **48**, 369–385.
44 M. Renz, M. Kess, M. Diedenhofen, A. Klamt and M. Kaupp, *J. Chem. Theory Comput.*, 2012, **8**, 4189–4203; S. Sinnecker, A. Rajendran, A. Klamt, M. Diedenhofen and F. Neese, *J. Phys. Chem. A*, 2006, **110**, 2235–2245.

